ESC European Society of Cardiology

European Heart Journal - Case Reports (2023) **7**, 1–6
https://doi.org/10.1093/ehjcr/ytad469

CASE REPORT
Heart failure

A long-term follow-up of necrobiotic xanthogranuloma with concomitant large-vessel vasculitis and heart failure with reduced ejection fraction: a case report

Naoto Setoguchi [1], Yukiteru Nakayama [1]*, Eisuke Amiya [1], Norifumi Takeda [1], and Issei Komuro [1,2]

[1]Department of Cardiovascular Medicine, The University of Tokyo, Tokyo, Japan; and [2]International University of Health and Welfare, Tokyo, Japan

Received 19 January 2023; revised 25 August 2023; accepted 19 September 2023; online publish-ahead-of-print 22 September 2023

Background Necrobiotic xanthogranuloma (NXG) is a non-Langerhans cell histiocytosis and multisystem disorder. Low level of HDL cholesterol associated with a systemic inflammatory profile, which may result from the interaction of monoclonal immunoglobulin and lipoproteins, is a characteristic feature. There is no evidence of NXG-associated large-vessel vasculitis, nor are there any established treatments, although chemotherapy for comorbid multiple myeloma is most often administered.

Case summary We describe a case of a 53-year-old male with a first history of heart failure with impaired systolic function. He presented with orbital xanthomas and multiple subcutaneous nodules, and laboratory examination showed elevated levels of C-reactive protein, low HDL, and paraproteinemia. A constellation of these clinical features and pathological findings of skin biopsy led to the diagnosis of NXG. ^{18}F-Fluorodeoxyglucose positron emission tomography (PET)/computed tomography (CT) confirmed increased uptake in the aorta and bilateral common carotid arteries. He began prednisolone treatment with reference to treatment for large-vessel vasculitis. After the treatment, C-reactive protein immediately decreased with markedly increased levels of apolipoprotein A1 (Apo-A1) and HDL. Systolic dysfunction was restored at 6-month follow-up. The patient has not experienced heart failure for 5 years after treatment, and the follow-up PET/CT demonstrated resolution of vascular inflammation.

Discussion This is the first report of NXG-associated large-vessel vasculitis. Low-dose prednisolone may benefit for NXG-associated vasculitis and cardiomyopathy. HDL, Apo-A1, and C-reactive protein levels may be useful for monitoring the activity of NXG, and PET/CT was a valuable diagnostic tool for NXG-associated vasculitis.

Keywords Case report • Large-vessel vasculitis • Heart failure with reduced ejection fraction • Necrobiotic xanthogranuloma

ESC curriculum 2.1 Imaging modalities • 6.2 Heart failure with reduced ejection fraction • 6.5 Cardiomyopathy • 9.1 Aortic disease

Learning points

- Necrobiotic xanthogranuloma (NXG) is associated with large-vessel vasculitis and cardiomyopathy.
- Low-dose prednisolone can restore cardiac function and repress the inflammation in the large vessels.
- Positron emission tomography/computed tomography evaluation is a valuable diagnostic tool in the imaging of NXG-associated vasculitis, and Apo-A1, HDL, and C-reactive protein would be useful for the management.

* Corresponding author. Tel: +81 3 3815 5411, Fax: +81 3 3818 6673, Email: m-ynakayama@g.ecc.u-tokyo.ac.jp
Handling Editor: Luke Joseph Laffin/Francesco Moroni
Peer-reviewers: Oliver Ian Brown, Massimo Mapelli, and Tisiana Felice
Compliance Editor: Nikolaos Spinthakis

Introduction

Necrobiotic xanthogranuloma (NXG) is a non-Langerhans cell histiocytosis and multisystem disorder first described by Kossard and Winkelmann in 1980.[1] Necrobiotic xanthogranuloma is characterized by low level of HDL and persistent paraproteinemia, yet the underlying mechanism remains elusive. We describe a case of NXG with large-vessel vasculitis and heart failure with reduced ejection fraction.

Summary figure

Time	Event(s)	Transthoracic echocardiography (TTE) findings
−10 years	Biopsy of the hepatic nodule showing a granulomatous lesion led to suspected tuberculosis	
−8 years	Diagnosed with multiple myeloma and treated with lenalidomide and prednisolone	Left ventricular end-diastolic dimension (LVDd) 48 mm, left ventricular ejection fraction (LVEF) 62%, trivial mitral valve regurgitation (MR)
−4 years	Lenalidomide and prednisone for multiple myeloma had been discontinued	
Day 0	Admission due to acute decompensated heart failure with severely impaired systolic function	LVDd 58 mm, LVEF 16%, severe MR
Day 14	Positron emission tomography/computed tomography (PET/CT) confirmed increased ^{18}F-fluorodeoxyglucose (^{18}F-FDG) uptake in the aorta and bilateral common carotid arteries	
Day 29	Initiation of prednisolone treatment (30 mg/day)	LVDd 58 mm, LVEF 26%, moderate MR
6 months	LVEF increased to 41% [cardiac magnetic resonance imaging (MRI)], and skin lesion was improved	
2 years		LVDd 56 mm, LVEF 44%, mild MR
3 years	Skin rashes relapsed with mild C-reactive protein elevation	
5 years	PET/CT showed decreased uptake in the aorta and cervical arteries	LVDd 51 mm, LVEF 38%, trivial MR

Case report

A 53-year-old Japanese male presented with worsening dyspnoea. Marked oedema was observed in the extremities, and chest radiography revealed pulmonary congestion. Transthoracic echocardiography showed a LVEF of 15%, biventricular diffuse hypokinesis, and left ventricular dilation with functional mitral regurgitation. He was hospitalized with a diagnosis of heart failure with reduced LVEF (HFrEF).

Ten years prior to the admission, he underwent liver biopsy for one hepatic mass, which showed a granulomatous lesion with Langerhans-type multinucleated giant cells and necrosis. Although *Mycobacterium tuberculosis* was not detected, he had been taking drugs against suspected tuberculosis. Eight years before the admission, he was diagnosed with multiple myeloma and treated with lenalidomide and prednisolone. The multiple myeloma subsequently settled down, and lenalidomide and prednisolone had been discontinued 4 years before admission. He had been followed up without hospitalization.

On admission, he presented with orbital xanthomas (*Figure 1A*) and subcutaneous nodules on the neck, trunk, and back (*Figure 1B*), which had been asymptomatic and uninvestigated since his childhood. Laboratory examination showed elevated levels of C-reactive protein, brain natriuretic peptide (BNP), high-sensitivity troponin I, and liver enzymes, and apolipoprotein A1 (Apo-A1) and HDL cholesterol were extremely low (see Supplementary material online, *Table S1*). Serum protein electrophoresis confirmed the presence of an IgGκ paraproteinemia. Urine immunoelectrophoresis indicated the presence of Bence Jones protein; however, bone marrow biopsy showed that plasma cells represented <10% of all nucleated cells, which did not meet the diagnostic criteria of multiple myeloma.

Computed tomography showed numerous plaques were accumulated from the aortic arch to the descending aorta (*Figure 2A*). Magnetic resonance angiography (MRA) showed prominent plaque formation, wall irregularities in bilateral common carotid arteries, and occlusion of left subclavian artery and left vertebral artery (*Figure 2B*). Coronary angiography demonstrated significant stenosis in the left anterior descending artery (LAD, *Figure 2C*), and the intravascular ultrasound confirmed diffuse hypoechoic plaques (*Figure 2D*). Right ventricular endomyocardial biopsy showed no obvious abnormalities. Cardiac MRI showed an inducible perfusion defect in extensive anterolateral region under adenosine triphosphate stress (*Figure 2E and F*). On the other hand, there was no evidence of myocardial oedema or late gadolinium enhancement (*Figure 2G*). Cardiac dysfunction was at least partly attributed to reduced blood flow in the coronary artery, and percutaneous coronary intervention was indicated for the LAD lesions; however, we prioritized optimal medical therapy due to the incidence of contrast-induced nephropathy after coronary angiography.

Advanced atherosclerotic lesions for his age, wall thickening of the aorta, and persistently elevated C-reactive protein level were highly suggestive of vasculitis. ^{18}F-Fluorodeoxyglucose PET/CT confirmed increased uptake in the aorta, bilateral common carotid arteries, and the skin area corresponding to the characteristic eruptions (*Figure 3D–F*).

He underwent skin biopsy of the eruption in the neck, which showed necrotic lesions from the dermis to the subcutaneous tissue, surrounded by inflammatory cell infiltration including foamy histiocytes (*Figure 4*). Cholesterin deposits and an infiltrate of foreign body-type polygonal giant cells that phagocytosed these deposits were also observed, and these were consistent findings with liver biopsy specimen 10 years ago.

He was finally diagnosed with NXG based on a constellation of his clinical and histopathological features. Necrobiotic xanthogranuloma is a non-Langerhans cell histiocytosis and multisystem disorder. Although the pathogenesis remains unknown, impaired macrophage

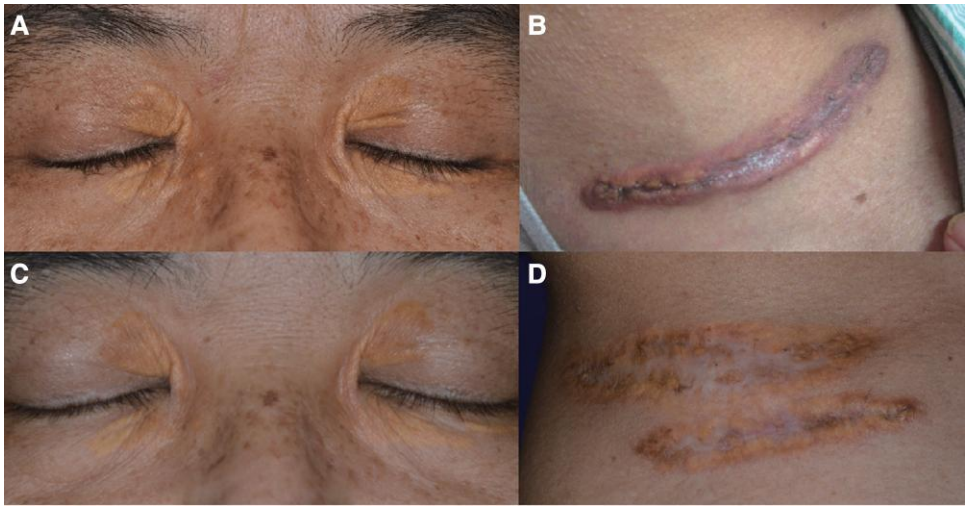

Figure 1 (*A*) Periorbital xanthoma on admission. (*B*) Neck ulcer on admission. (*C*) Periorbital xanthoma after prednisolone administration (Day 198). (*D*) Neck ulcer after prednisolone administration (Day 198).

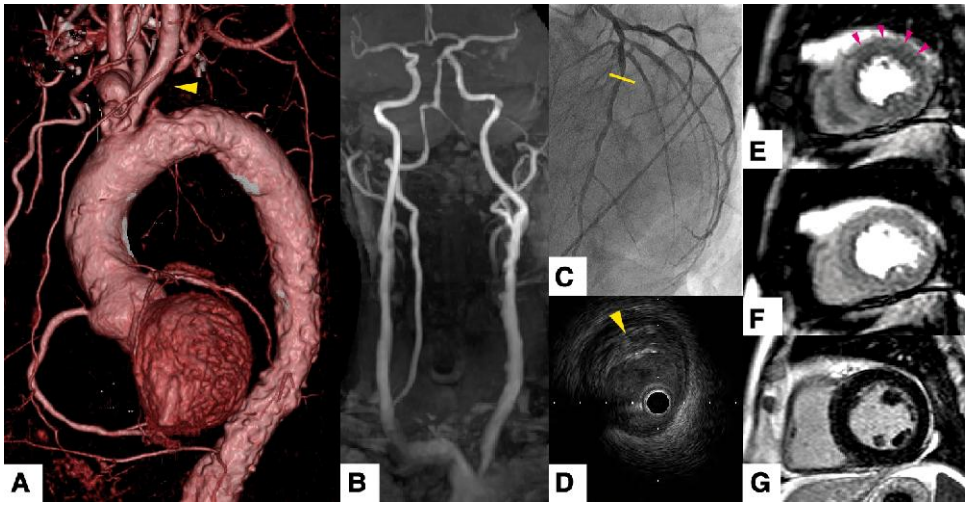

Figure 2 (*A*) Three-dimension reconstruction of computed tomography showed aortic plaque and left subclavian artery occlusion (arrowhead). (*B*) Non-contrast enhanced magnetic resonance angiography showed prominent plaque formation, wall irregularities in bilateral common carotid arteries, and occlusion of the left vertebral artery. (*C*) Coronary angiography in left anterior oblique cranial view showed stenosis in the left anterior descending artery (line). (*D*) Intravascular ultrasound of the left anterior descending artery confirmed diffuse hypoechoic plaques (arrowhead). (*E*) Cardiac magnetic resonance of adenosine triphosphate stress perfusion and (*F*) rest perfusion showed an inducible perfusion defect in extensive anterolateral region (arrowhead). (*G*) Cardiac magnetic resonance imaging showed no obvious late gadolinium enhancement.

lipid homeostasis associated with a systemic inflammatory profile, which may result from the interaction of monoclonal immunoglobulin and lipoproteins, and extremely low levels of HDL are characteristic features.[2] He began prednisolone treatment with at an initial dose of 0.5 mg/kg/day (30 mg/day) with reference to treatment for large-vessel vasculitis. After the treatment, skin yellow rashes became thinner (*Figure 1C and D*), and C-reactive protein immediately decreased with markedly increased levels of Apo-A1 and HDL (*Figure 5*). In addition to prednisolone, carvedilol, and enalapril as a guideline-directed medical therapy (GDMT) for HFrEF at the time, aspirin and rosuvastatin for ischaemic heart disease were introduced. Brain natriuretic peptide level also decreased promptly and ST-T abnormalities of electrocardiogram on admission gradually improved (see Supplementary material online,

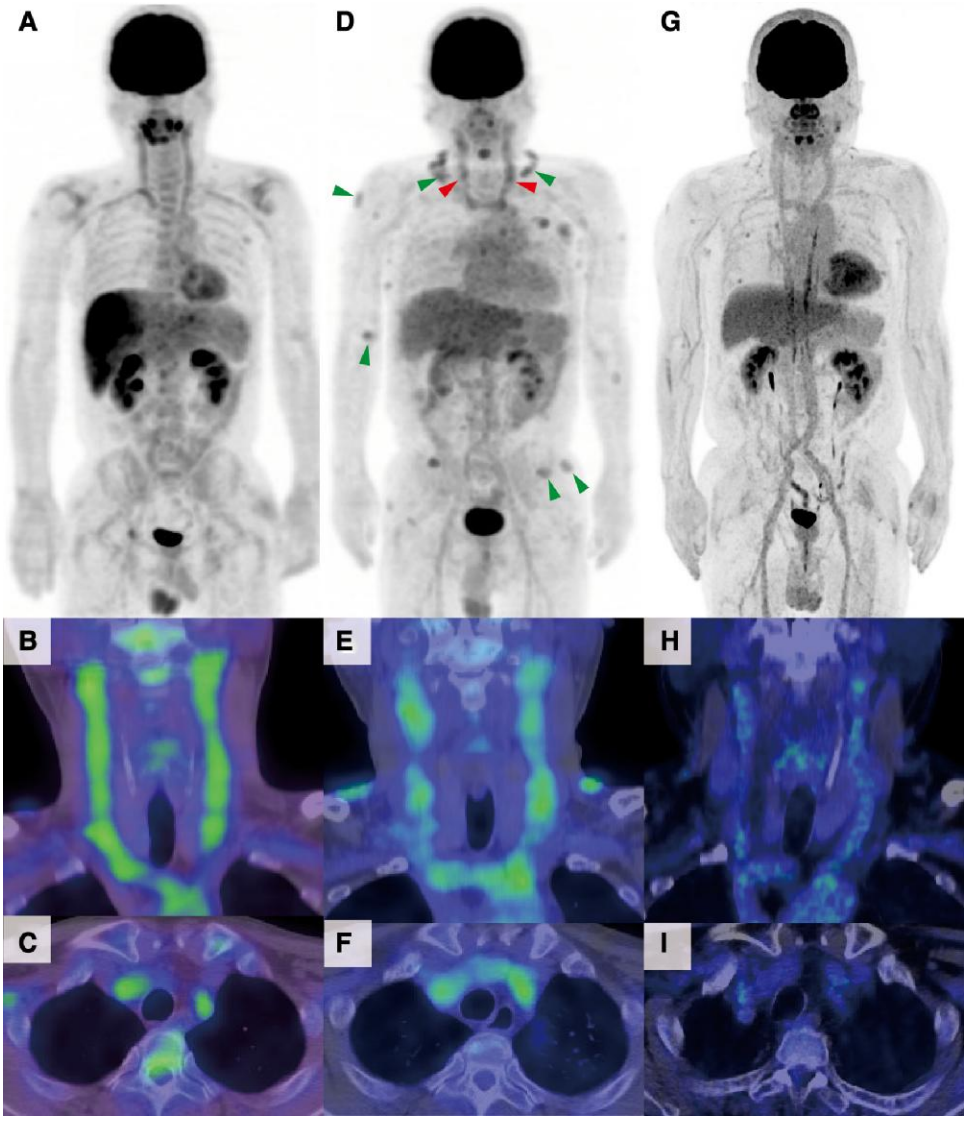

Figure 3 (*A–C*) Positron emission tomography/computed tomography 10 years before diagnosis. A total of 223 MBq of ^{18}F-fluorodeoxyglucose was administered (5-h fasting). (*A*) The maximal intensity projection showed fluorodeoxyglucose uptake in bilateral common carotid arteries (maximum standardized uptake value: SUVmax 3.2). (*D–F*) Positron emission tomography/computed tomography on admission. A total of 275 MBq of ^{18}F-fluorodeoxyglucose was administered (20-h fasting). (*D*) The maximal intensity projection showed fluorodeoxyglucose uptake in bilateral common carotid arteries (SUVmax 3.1, red arrowhead) and fluorodeoxyglucose uptake corresponding to the skin lesions (green arrowhead). (*G–I*) Latest positron emission tomography/computed tomography after 296 MBq of ^{18}F-fluorodeoxyglucose was administered (5-h fasting). (*G*) The maximal intensity projection showed dampened uptake in bilateral common carotid arteries and skin lesions. (*B*, *E*, *H*) Coronal section of the carotid arteries. (*C*, *F*, *I*) Axial section at the level of the brachiocephalic trunk.

Figure S1). Left ventricular ejection fraction increased to 41% at 6-month follow-up.

Three years after the treatment, when prednisolone tapered to 5 mg/day, skin rashes relapsed with mild C-reactive protein elevation. Prednisolone dose was increased to 20 mg/day and tapered slowly to the maintenance dose of 8 mg/day. Thereafter, no relapse of skin rashes or C-reactive protein elevation was observed for 3 years. According to the updated GDMT, he is currently taking carvedilol 10 mg, sacubitril valsartan 100 mg, dapagliflozin 10 mg, and rosuvastatin 2.5 mg daily and receives 140 mg of evolocumab every 2 weeks as well. His HDL and Apo-A1 levels remain high despite the persistent paraproteinemia and M-proteinemia. Although LVEF has not recovered completely, his BNP level maintains low (*Figure 5*). The PET/CT obtained 5 years after treatment demonstrated decreased uptake in the aorta and cervical arteries, reflecting the resolution of vascular inflammation (*Figure 3G–I*).

Discussion

We experienced a case of NXG with large-vessel vasculitis and HFrEF. Optimal medical therapy combined with low-dose prednisolone drastically restored cardiac function, and the inflammation in the large

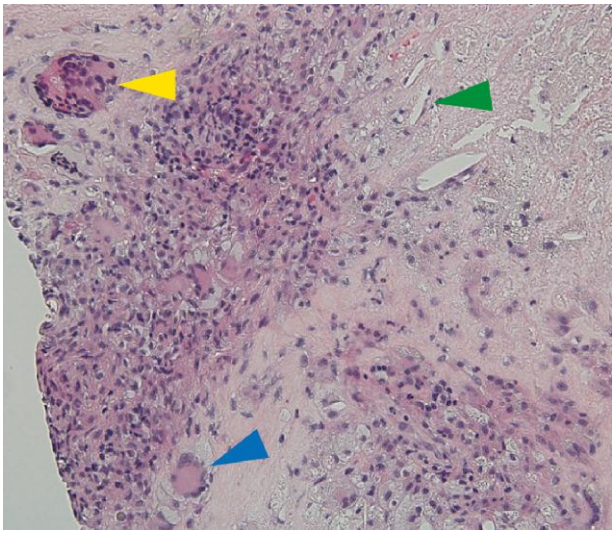

Figure 4 Dermatopathological findings (haematoxylin and eosin, magnitude × 200) showed necrotic lesions, surrounded by inflammatory cell infiltrations containing foamy histiocytes and foreign body giant cell (yellow arrowhead). Cholesterin cleft (green arrowhead) and Touton giant cell (blue arrowhead) were also observed.

vessels was repressed. Cardiac manifestations of NXG have been reported; however, a limited number of studies have been reported on NXG-associated vasculitis, and there is no evidence to suggest direct involvement in large-vessel inflammation.[1,3–6] Treatment for NXG varies greatly depending on the clinical features and severity, and chemotherapy for haematological disorders including multiple myeloma is most often administered.[7,8] In the present case, low-dose prednisolone was administered in accordance with the treatment for large-vessel vasculitis because his paraproteinemia did not meet the treatment criteria for multiple myeloma. Low-dose prednisolone drastically restored the status of heart failure and improved lipid profile, which to the best of our knowledge have not been reported before. Additionally, HDL and Apo-A1 levels remained high despite the persistent paraproteinemia and M-proteinemia. This suggests that prednisolone cannot prevent production of monoclonal immunoglobulin by plasma cells nor the interaction with lipoproteins but curb the consumption of Apo-A1 by repressing inflammation. Apo-A1, HDL, and C-reactive protein would be useful for the management of NXG and NXG-associated vasculitis.

The PET/CT was sensitive for the detection of large-vessel vasculitis on admission, while aortic ^{18}F-FDG uptake could be detected also 10 years before the diagnosis of NXG (*Figure 3A–C*); however, these findings had been left unexplored due to a lack of the apparent symptom until incidental heart failure. The present case might suggest NXG remains underinvestigated or underdiagnosed in many cases, and thus, further investigation is crucial to identify patients with vasculitis who may benefit from low-dose prednisolone; PET/CT evaluation should

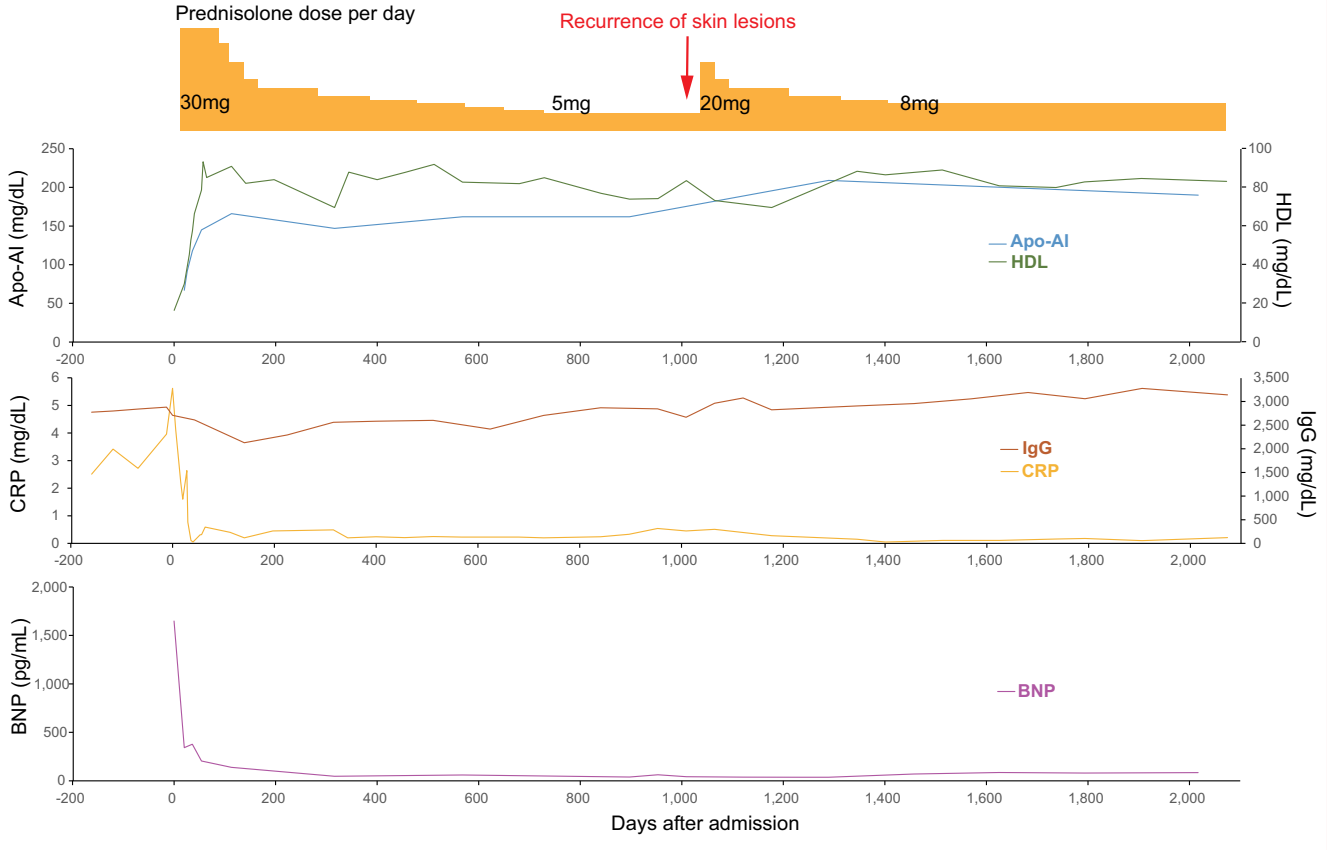

Figure 5 The patient's therapeutic course. C-reactive protein and brain natriuretic peptide levels immediately decreased after the treatment of prednisolone, while Apo-A1 and HDL levels were increased from an abnormally low level to the upper reference limit. An abnormally high level of IgG persisted irrespective of the prednisolone.

be an essential diagnostic tool in the imaging of cardiovascular inflammation.

Lead author biography

Naoto Setoguchi graduated from Yamaguchi University in 2016. In 2018, he completed his junior residency programme at the University of Tokyo Hospital. From 2018 to 2022, he worked as a senior resident at Mitsui Memorial Hospital. Currently, he is working as a graduate student at the Department of Cardiovascular Medicine, University of Tokyo Hospital.

Supplementary material

Supplementary material is available at *European Heart Journal – Case Reports* online.

Consent: Written informed consent in accordance with COPE guidelines was obtained from the patient.

Conflict of interest: None declared.

Funding: This work was supported by Japan Society for the Promotion of Science (grant number 21K08122).

Data availability

The data underlying this article are available in the article and in its online supplementary material.

References

1. Kossard S, Winkelmann RK. Necrobiotic xanthogranuloma*. *Aust J Dermatol* 1980;**21**:85–88.
2. Szalat R, Pirault J, Fermand JP, Carrie A, Saint-Charles F, Olivier M, *et al.* Physiopathology of necrobiotic xanthogranuloma with monoclonal gammopathy. *J Intern Med* 2014;**276**:269–284.
3. Novak PM, Robbins TO, Winkelmann RK. Necrobiotic xanthogranuloma with myocardial lesions and nodular transformation of the liver. *Hum Pathol* 1992;**23**:195–196.
4. Winkelmann RK, Litzow MR, Umbert IJ, Lie JT. Giant cell granulomatous pulmonary and myocardial lesions in necrobiotic xanthogranuloma with paraproteinemia. *Mayo Clin Proc* 1997;**72**:1028–1033.
5. Szalat R, Arnulf B, Karlin L, Rybojad M, Asli B, Malphettes M, *et al.* Pathogenesis and treatment of xanthomatosis associated with monoclonal gammopathy. *Blood* 2011;**118**:3777–3784.
6. Hou J, Long T, Hu S. Application of 18F-FDG PET/CT in necrobiotic xanthogranuloma involving multiple organs. *Eur J Nucl Med Mol Imaging* 2021;**48**:321–322.
7. Nelson CA, Zhong CS, Hashemi DA, Ashchyan HJ, Brown-Joel Z, Noe MH, *et al.* A multicenter cross-sectional study and systematic review of necrobiotic xanthogranuloma with proposed diagnostic criteria. *JAMA Dermatol* 2020;**156**:270–279.
8. Miguel D, Lukacs J, Illing T, Elsner P. Treatment of necrobiotic xanthogranuloma—a systematic review. *J Eur Acad Dermatol Venereol* 2017;**31**:221–235.